

Sensitivity dependent model of protein-protein interaction networks

Jingshan Zhang and Eugene I. Shakhnovich
 Department of Chemistry and Chemical Biology,
 Harvard University, Cambridge, Massachusetts 02138
 (Dated: March 29, 2024)

The scale free structure $p(k) \sim k^{-\gamma}$ of protein-protein interaction networks can be reproduced by a static physical model in simulation. We inspect the model theoretically, and find the key reason for the model to generate apparent scale free degree distributions. This explanation provides a generic mechanism of "scale free" networks. Moreover, we predict the dependence of γ on experimental protein concentrations or other sensitivity factors in detecting interactions, and find experimental evidence to support the prediction.

1. Introduction

"Scale free" networks have been observed in many areas of science [1] including social science, biology and internet, where degree distributions follow (albeit noises) the power law form $p(k) \sim k^{-\gamma}$ within one or two orders of magnitude for k . Here the degree k is the number of links a node has, and $p(k)$ is the probability of a node to have degree k . An important scale free network under experimental [2, 3, 4, 5] and theoretical [1, 6, 7, 8, 9, 10, 11, 12, 13] study is the protein-protein interaction (PPI) network, where a link between two proteins indicates a large enough binding energy between them. These studies bare the goal that the topology of PPI networks could reflect how systems of various proteins have evolved in biological organisms.

It was pointed out recently that scale free PPI networks could also result from variation of surface hydrophobicities of proteins. Starting from an approximately Gaussian distribution of surface hydrophobicity, the static model successfully produced scale free networks in computer simulations [6].

Why can this static model generate scale free networks? As a counterpart of the simulation results in Ref. [6], in this paper we study the model from a theoretical perspective, and reveal the key reason that the model leads to "scale free" networks. More importantly, our numerical and analytical study reveals the dependence of power γ on experimental sensitivity factors, such as protein concentration, in detection of PPI, and provides a possible explanation to the observed variation of γ in different high-throughput PPI experiments.

2. The static model

Let us first briefly introduce the model proposed by Deeds et al. [6]. For the compositions of surface residues of yeast proteins in high-throughput experiments [3, 4], the fractions of hydrophobic residues, noted as p , follow a Gaussian distribution

$$f(p) = \frac{1}{\sqrt{2\pi}} e^{-\frac{(p-\bar{p})^2}{2\sigma^2}} \quad (1)$$

with mean value $\bar{p} = 0.2$ and deviation $\sigma = 0.05$. This results in an approximately Gaussian distribution of the

surface "stickiness" K , and the binding free energy of two proteins is determined by the sum of their "stickiness". In a more detailed description, there are K_i hydrophobic residues among the M surface residues on protein i , and $M = 100$ is assumed to be a constant for all proteins. The probability to find a protein with K hydrophobic surface residues is

$$p_E(K) = \int_0^1 dp f(p) \binom{M}{K} p^K (1-p)^{M-K} \quad (2)$$

It can be seen that $p_E(K)$ is close to a Gaussian distribution (Fig. 1a).

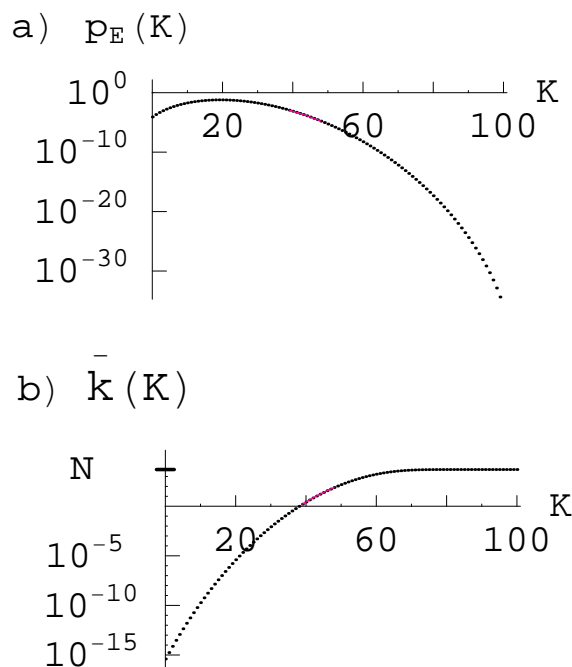


FIG. 1: (color online). a) Hydrophobicity distribution $p_E(K)$ in Eq. (2) for $N = 5000$. The K region in red is the same as in the inset. b) The dependence of expected degree \bar{k} upon hydrophobicity K , for $K_c = 83$. The range $1 \leq \bar{k} \leq 100$ is in red.

The binding of protein i and j is determined by the

binding free energy

$$G = (K_i + K_j)F_0 + G_{(0)}; \quad (3)$$

where G is negative for a strong binding, F_0 is the change of binding free energy upon burial of each hydrophobic residue, and $G_{(0)} \approx 6 \text{ kcal/mol}$ at 10 k_B T is a constant value determined by experiments [14, 15]. In support of this model, Fig. 3 of Ref. [14] showed that experimental result of binding energies can be described by the sum of stickiness terms and a constant term. If $K_i + K_j > K_c$ the interaction is experimentally detectable, and the two proteins are labeled as linked in the PPI network.

3. Results and interpretations

3.1. Degree distributions

We calculate $p(k)$ numerically (see Numerical method for details) with given values of N and K_c , where N is the total number of proteins in the network, and obtain apparent "scale free" structure $p(k) \sim k^{-2}$ (Fig. 2). We set the default situation as $N = 5000$ and $K_c = 83$ to $t = 2$. Fig. 2 indicates that the apparent slope increases with K_c , and increases as N decreases. More explicitly, the dependence of γ upon K_c is plotted in Fig. 3.

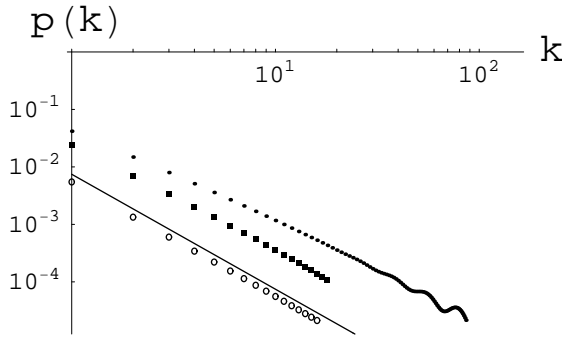


FIG. 2: "Power law" degree distribution $p(k)$ for different situations, with a solid line indicating slope $= 2$. Circles (default): $N = 5000$ and $K_c = 83$; dots: $N = 5000$ and $K_c = 75$; squares: $N = 1000$ and $K_c = 75$. Only data with $p(k) > \frac{1}{10N}$ are shown.

Let us interpret these results by analytical approaches. A protein with hydrophobicity K has a pass/fail line

$$K_{\text{line}} = K_c - K; \quad (4)$$

Proteins with hydrophobicity above K_{line} are linked to it, while those with hydrophobicity below K_{line} do not. Therefore the protein with hydrophobicity K has an average degree

$$\bar{k} = N \int_{K_{\text{line}}}^{\infty} p_e(K) dK \quad (5)$$

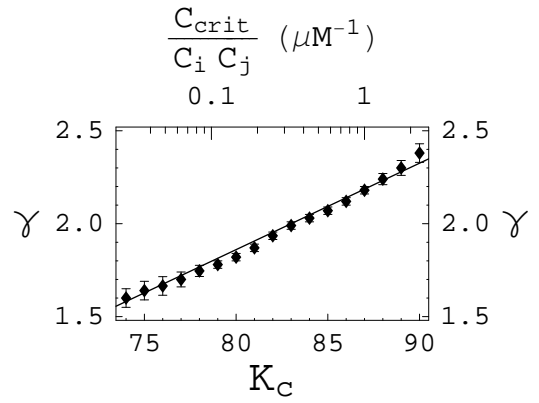


FIG. 3: Dependence of the power-law index upon experimental sensitivity in detecting interactions. γ increases with K_c , and K_c is replaced on the top by $\frac{C_{\text{crit}}}{C_i C_j}$ from Eq. (12). The error bar at $K_c = 78$ comes mostly from undulations. The slight γ at $K_c = 1$ produces bigger error bar at $K_c = 88$ where there are less data points. The solid line is the approximation Eq. (9).

In the mean-field approximation the degree of the protein k is just \bar{k} , and the degree distribution is

$$p(\bar{k}) = p_e(K) \frac{dK}{d\bar{k}} = \frac{p_e(K)}{N p_e(K_c - K)}; \quad (6)$$

Beyond mean-field approximation its degree fluctuates with deviation \bar{k} , which will be addressed later.

Let us restrict the discussion within the mean-field approximation for the moment. We can notice that the experimentally observable range $1 \leq k \leq 100$ only covers a small range of hydrophobicity ($39 \leq K \leq 48$ for the default situation), as indicated by the short red line in Fig. 1b. In this range the hydrophobicity distribution $p_e(K)$ is very close to exponential, since the short red line in Fig. 1a is nearly straight. So we can use linear approximation to produce the nearly straight lines in Fig. 2. Define

$$a, \quad \frac{d \ln p_e(K)}{dK} \bigg|_{K=K_0} = -\frac{1}{K_{\text{line}}} \quad (7)$$

and

$$b, \quad \frac{d \ln p_e(K)}{dK} \bigg|_{K=K_0} = -\frac{1}{K_c}; \quad (8)$$

then Eq. (5) give $\bar{k} = e^{aK + \text{const}}$, while Eq. (6) leads to $p(\bar{k}) = e^{-(a+b)K + \text{const}}$. As a result we have $p(\bar{k}) \sim \bar{k}^{-(1+b/a)}$. This is a "scale free" network with $\gamma = 1 + b/a$.

To understand the undulations in $p(k)$ at large k in Fig. 2, we must go beyond the mean-field approximation and deal with the fluctuation of degree with magnitude \bar{k} for a given \bar{k} . Noticing the K values are discrete integers, each K value produces a peak in $p(k)$, centered at \bar{k} and with width $\sim \bar{k}$. Since \bar{k} grows with K almost exponentially, the distance between nearest neighbor peaks

$\bar{k}(K+1) - \bar{k}(K)$ grows linearly with \bar{k} . The undulations emerge at large enough \bar{k} , when the peak distance exceeds the peak width \bar{k} .

Now we are ready to study the dependence of the slope on parameter K_c in Fig. 3. Approximating the hydrophobicity distribution as Gaussian distribution $\ln p_e(K) \propto -(K - K_0)^2$, where K_0 is the most probable hydrophobicity value, we have

$$= 1 + \frac{b}{a} \left(1 + \frac{K_c - K_{line} - K_0}{K_{line} - K_0} \right); \quad (9)$$

We find $K_0 \approx 20$ in Eq. (2), and $K_{line} \approx 41.5$ is nearly a constant from Eq. (5) for typical degree $k \approx 5$, then $\ln p_e(K)$ is a linear function of K_c in Eq. (9), and forms a straight line (solid) in Fig. 3.

3.2. Dependence on experimental sensitivity

Different values have been obtained in different PPI experiments, varying from 2:1 to 2:5 [3, 4, 5, 8, 9, 10]. To explain this variation, we notice that different experiments might have different sensitivity in detecting PPI. Indeed, some interactions detectable in one experiment might be too weak to be detected in another experiment. An example of factors affecting experimental sensitivity is protein concentration/level, which is in turn controlled by gene expression and dependent upon the specific technique used to detect PPI. Even for the same experiment, the sensitivity in detecting interactions is actually reduced by setting a higher standard in identifying PPI, e.g., selecting only highly repeatable PPI data which effectively correspond to interactions with high affinity.

Let us study how \bar{k} depends on these experimental sensitivity factors. In high-throughput experiments the concentration of protein-protein complex C_{ij} must be high enough to be detected

$$C_{ij} = \frac{C_i C_j}{C_0} \exp \left(-\frac{G}{k_B T} \right) > C_{crit}; \quad (10)$$

where the binding free energy G is given by Eq. (3), C_i and C_j are the concentrations of proteins i and j in monomeric form, and the normalization concentration $C_0 = 1M$ is the convention. Rewriting this relationship in the form of association constant, the binding affinity should be strong enough to be detectable

$$K_a = \frac{1}{C_0} \exp \left(\frac{(K_i + K_j)F_0 - G_{(0)}}{k_B T} \right) > \frac{1}{C_0} \exp \left(\frac{K_c F_0 - G_{(0)}}{k_B T} \right) = \frac{C_{crit}}{C_i C_j}; \quad (11)$$

Thus the parameter K_c of the model is determined by experimental protein concentrations

$$K_c = k_B T \ln \left(\frac{C_0 C_{crit}}{C_i C_j} \right) + G_{(0)} = F_0; \quad (12)$$

To estimate the only unknown parameter F_0 in this equation, we notice that for yeast two hybrid screening technique the PPIs with binding affinity $K_a > \frac{C_{crit}}{C_i C_j} \approx 1 M^{-1}$ are detectable [16]. If we use 2:3 and $K_c = 87$ for this threshold binding affinity, we can obtain an estimate $F_0 \approx 0.28 k_B T$. With the help of this value we can use Eq. (12) to convert the x-axis of Fig. 3 from K_c to experimental variable $\frac{C_{crit}}{C_i C_j}$ (top of Fig. 3).

It can be seen from Fig. 3 that lower sensitivity, or lower $C_i C_j$, leads to higher \bar{k} . This can be realized by lower protein concentrations through reduced gene expressions, or selecting only highly repeatable data of detected PPIs. This prediction is confirmed by Figure 2a of Ref. [10], which clearly shows that the core data set of Ito et al. [4], containing only PPIs identified by at least three independent sequence tags, generates a steeper degree distribution than the full Ito data set does. Obviously the Ito core data corresponds to relatively strong interactions, manifest in high K_a and K_c . Note that the horizontal dots with $p(k) = 1/N$ at high k in Figure 2a of Ref. [10] should be excluded when fitting the slope, because they are actually in the $p(k) < 1/N$ region where a few nodes with arbitrary degree k emerge occasionally. On the other hand, the protein concentrations in the yeast two hybrid experiments [3, 4] are not yet available, and the prediction about dependence of the slope upon protein concentration needs verification from future experiments.

3.3. Clustering coefficient

We also study another important property of networks, clustering coefficient $C(k)$, and show the numerical result of the model in Fig. 4. If a protein is linked to k proteins, the average number of links between the k proteins, $t(k)$, cannot exceed $k(k-1)/2$. Here the averaging includes all possible realizations. The clustering coefficient is $C(k) = \frac{2t(k)}{k(k-1)} \leq 1$. Similarly to Ref. [17, 18], we obtain (Fig. 4) $C(k) \approx 1$ at small k and $C(k) \propto k^{-2}$ at large k . The experimental result [2, 3, 4, 10] has a similar shape with slope -2 for large k , and $C(k)$ is smeared between 1 and 10^{-1} for small k . If we attribute the discrepancy between the model and experiment at small k to false negatives, the model is in reasonable agreement with experiments.

A physical picture is helpful to interpret this result. As mentioned above, if there are the k proteins linking to the same protein, their hydrophobicity exceed K_{line} , while the hydrophobicity of all other proteins are below K_{line} . The mean field relationship between K_{line} and k is Eq. (5). If we have $K_{line} - K_c = 2$ at a small degree k , then the most hydrophobic k proteins are all connected, and $C(k)$ is 1. At large enough k , however, $K_{line} < K_c = 2$ and not all proteins above K_{line} are linked to each other. Then the clustering coefficient is determined by

$$C(k) \approx \frac{\int_{K_{line}}^{K_c} \frac{R_M}{K_{line}} dK_1 \int_{K_{line}}^{K_c} \frac{R_M}{K_{line}} dK_2 p_e(K_1) p_e(K_2)}{\int_{K_{line}}^{K_c} \frac{R_M}{K_{line}} dK_1 \int_{K_{line}}^{K_c} \frac{R_M}{K_{line}} dK_2 p_e(K_1) p_e(K_2)}; \quad (13)$$

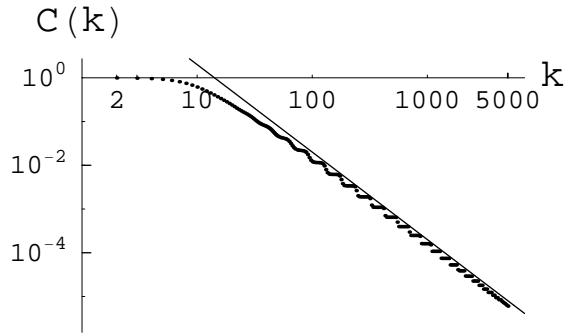


FIG. 4: The clustering coefficient distribution $C(k)$ for the default situation. The solid line indicates slope -2 .

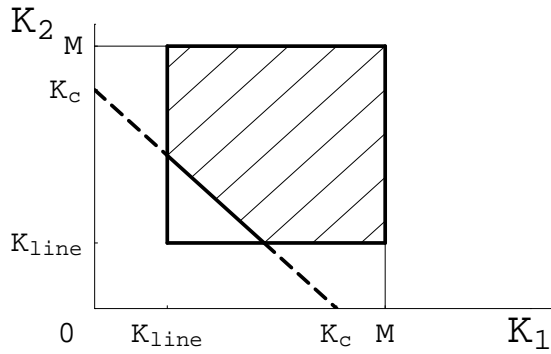


FIG. 5: The diagram of Eq. (13) to find the behavior of clustering coefficient $C(k)$. The numerator is the integral over the shadowed region, while the denominator is the integral over the square region.

The denominator is proportional to \bar{k}^2 according to Eq. (5). It corresponds to the square region between K_{line} and M in Fig. 5. The numerator, corresponding to the shadowed region in Fig. 5, is dominated by the region near the cutting line $K_1 + K_2 = K_c$, because $p_e(K)$ is nearly a sharp exponential function. Hence the numerator scales as the length of the cutting line, $K_c - 2K_{line} / \ln \bar{k} + \text{const.}$ Therefore, in agreement with Boguna et al. [18], the numerator is a slow function of k compared to the denominator, and the clustering coefficient scales as $C(\bar{k}) \sim \bar{k}^{-2}$ at large \bar{k} . And at small \bar{k} the square is totally in the shadow, leading to $C(\bar{k}) \sim 1$. The step like shape of $C(k)$, however, comes from the discreteness of integer K values.

4. Numerical methods

We calculate $p(k)$ as an average of all possible realizations. The calculation is done with integer K^0 and without mean field approximation. We ignore the unimportant difference between N and $N + 1$ for large

enough N . The exact form of Eq. (5) is

$$\bar{k} = N \sum_{K^0=0}^M p_e(K^0) \quad (14)$$

and the degree distribution is

$$p(k) = \sum_{K=0}^M p_e(K) \frac{N}{k} (\bar{k} - N)^k (1 - \bar{k} - N)^{N-k} \quad (15)$$

Instead of mean field result Eq. (13), the clustering coefficient is calculated as

$$C(k) = \frac{\sum_{K=0}^M \sum_{K_1+K_2=K} p_e(K_1)p_e(K_2)}{[\sum_{K_1+K_2=K} p_e(K_1)p_e(K_2)]} \quad (16)$$

where

$$f(K) = \begin{cases} 1 & K > 0 \\ 0 & K < 0 \end{cases} \quad (17)$$

is the usual Heaviside step function, and

$$w(K) = \sum_{K^0=K}^N \left[\sum_{K^0=0}^K p_e(K^0) \right]^k f \left[\sum_{K^0=0}^{K-1} p_e(K^0) \right]^{N-k} \left[\sum_{K^0=0}^{K-2} p_e(K^0) \right]^{N-k} g \quad (18)$$

is the probability that k proteins have hydrophobicity K while the maximum hydrophobicity of the rest $N - k$ proteins is $K - 1$.

5. Conclusion and outlook

We study a static physical model to explain scale free PPI networks. We notice that the experimentally observable part of degree distribution covers a limited range (from $k = 1$ to $k < 100$), and corresponds to a small range of hydrophobicity. The hydrophobicity distribution $p_e(K)$ in this small range is close enough to an exponential distribution. Therefore a linear approximation leads to the "scale free" degree distribution $p(k) \sim k^{-2}$, with \bar{k} dependent on the threshold parameter K_c and network size N . In experiments K_c depends on the sensitivity factors, such as protein concentration, in detection of PPI. Our result provides a possible interpretation to the difference in experimental values, and predicts the dependence of \bar{k} on experimental sensitivity factors. This prediction is supported by the slope change [10] when comparing Ito data set and Ito core data set [4], and dependence of \bar{k} on protein concentrations needs experimental verification in future. The distribution of another network property, clustering coefficient, produced in the model is also in reasonable agreement with that of experiment [10] and previous theoretical descriptions [17, 18].

The hydrophobicity distribution in the physical model has been arranged to reflect the reality in a simplified way. While the real distribution of protein "stickiness" can be somewhat different from it, the generation of "scale free" network will not be sensitive to the difference. More generally, "scale free" degree distributions can be also produced by many smooth distributions of hydrophobicity, such as binomial, Gaussian, Poisson distributions and their modifications. This can be one of the reasons that scale free (in a limited range) networks are so widely observed.

A major part of PPI networks is obtained by the high-throughput yeast two hybrid screening [3, 4]. This technique often produces a large fraction of false positives [19] which do not correspond to any real biological function, while real functional interactions presumably constitute a smaller portion of the detected result. While functional PPI may involve formation of additional hydrogen bonds and salt bridges to obtain adequate binding affinity, these nonfunctional PPIs have not been evolutionarily selected and are formed primarily due to hydrophobic effect. In this model we show that a simple static network of nodes with different "stickiness" can readily appear to be scale free. To this end, we use Eq. (3) because the nonfunctional PPIs are just random interfaces between two proteins without experiencing the evolutionary design of pairwise interface patterns. Moreover, this model could be used to extract information of nonfunctional interactions between unrelated proteins which randomly encounter in a real cell, and such information is in turn important in probing the general principles for cells to organize proteins in a cell. Namely, the stronger nonfunctional interactions, the more unrelated proteins interfere with each other, and the less protein types can coexist. Hence the nonfunctional interactions can limit the proteome size of a single cellular organism. Interesting related questions include the change of how much living cells have to do in constricting the nonfunctional interactions in the course of protein evolution, as well as the impact of higher temperature for thermophilic organisms.

If the distribution of "stickiness" is simply an exponential function, $\ln p_i(K) = -K$, the model is simplified to $a = b$ and $\gamma = 2$. This reduced simple situation would then be in complete agreement with one of the mathematical examples of networks briefly mentioned in by Caldarelli et al. [20], which has been applied to realistic networks such as gene regulation network [21]. Our finding indicates that this simple mathematical form [20] have more important impacts to systems in reality. Indeed, it is reasonable to expect distribution of many qualities, such as annual personal income and eagerness to learn knowledge, to be fitted by an approximately exponential distribution at least in some short range, and with suitable arrangements power law distribution might emerge.

Masuda et al. [17] followed the suggestion of Caldarelli et al. [20] and studied essentially similar models to ours. But they did not relate the mathematical models to real

systems. More importantly, they emphasize that the slope $\gamma = 2$ is universal, while the slope in our study not only deviates from 2, but also depends on experimental properties such as expression levels of proteins.

In contrast to this static model, most models of PPI networks focus on the development history of the network through gene duplications [11, 12], which is similar to "preferential attachment" in growing networks [13]. It was found [12] that the network structure of the gene duplication model analytically approaches scale free [12] at $k \gg 1$ if links of new nodes should be deleted by a probability larger than $1/2$, and the degree distribution is comparable with experiments. Our approach serves as an alternative way to obtain "scale free" PPI network. Further experiments, such as systematic study of dependence of apparent power γ on gene expression level, or other measures of protein concentration, will help clarify whether the static model or gene duplication mechanism is mainly responsible for the observed scale free nature of PPI networks.

Glossary

Protein-protein interaction network. A network of many types of proteins of an organism; each type of protein is a node in the network. Two nodes are labeled as linked if the two types of proteins can interact with each other with sufficient affinity.

Degree. The number of links a node has in the network. If a node in the protein-protein interaction network has degree k , this protein can interact with k other types of proteins.

Scale free network. In such a network, the number of nodes with degree k decreases with k , and the dependence is a power law function.

Yeast two hybrid. A molecular biology technique used to discover protein-protein interactions by testing for physical interaction/binding between two proteins, respectively. This technique is able to test interactions between a large amount of proteins rapidly (so called high-throughput screening).

sensitivity in detecting interactions. Only strong enough interactions between proteins are identified as "interacting" pairs. If the sensitivity in detection becomes higher, slightly weaker interactions become detectable, and more interactions are detected.

Surface hydrophobicity. The fraction of hydrophobic amino acids among the amino acids on the surface of a protein. If hydrophobic amino acids are buried either in formation of a protein or in formation of a protein-protein complex, they are not in contact with water any more, and thus lowers the total free energy. Hydrophobic effect is important in the interac-

tion of proteins, especially in non-functional interactions.

Acknowledgement: This work is supported by NIH.

-
- [1] R. Albert and A.-L. Barabási, Statistical mechanics of complex networks, *Review of Modern Physics* 74, 47 (2002).
- [2] I. Xenarios, D. W. Rice, L. Salwinski, M. K. Baron, E. M. Marcotte, D. Eisenberg, DIP: the Database of Interacting Proteins, *Nucleic Acids Res.* 28, 289 (2000); H. W. Mewes, D. Frishman, U. Guldener, G. Mannhaupt, K. Mayer, M. Mokrejs, B. Morganstem, M. Munsterkotter, S. Rudd, B. Weill, MIPS: a database for genomes and protein sequences, *Nucleic Acids Res.* 30, 31 (2002).
- [3] P. Uetz, L. Giot, G. Cagney, T. A. Mansfield, R. S. Judson, J. R. Knight, D. Lockshon, V. Narayan, M. Srinivasan, P. Pochart, et al., A comprehensive analysis of protein-protein interactions in *Saccharomyces cerevisiae*, *Nature (London)* 403, 623 (2000);
- [4] T. Ito, K. Tashiro, S. Muta, R. Ozawa, T. Chiba, M. Nishizawa, K. Yamamoto, S. Kuhara, Y. Sakaki, Toward a protein-protein interaction map of the budding yeast: A comprehensive system to examine two-hybrid interactions in all possible combinations between the yeast proteins, *Proc. Natl. Acad. Sci. USA* 97, 1143 (2000); T. Ito, T. Chiba, R. Ozawa, M. Yoshida, M. Hattori, and Y. Sakaki, A comprehensive two-hybrid analysis to explore the yeast protein interactome, *Proc. Natl. Acad. Sci. USA* 98, 4569 (2001).
- [5] J. F. Rual, K. Venkatesan, T. Hao, T. Hirozane-Kishikawa, A. Dricot, N. Li, G. F. Bertozzi, F. D. Gibbons, M. Doree, N. Aiyi, G. Uedehoussou, et al., Towards a proteome-scale map of the human protein-protein interaction network, *Nature (London)* 437, 1173 (2005); J. Lin, T. Hao, C. Shaw, A. J. Patel, G. Szabo, J. F. Rual, C. J. Fisk, N. Li, A. Smolyar, D. E. Hill, et al., A protein-protein interaction network for human inherited ataxias and disorders of Purkinje cell degeneration, *Cell* 125, 801 (2006).
- [6] E. J. Deeds, O. Ashenberg, and E. I. Shakhnovich, A simple physical model for scaling in protein-protein interaction networks, *Proc. Natl. Acad. Sci. USA* 103, 311 (2006).
- [7] Y. Shi, G. Miller, H. Qian, and K. Bom sztyk, Free-energy distribution of binary protein-protein binding suggests cross-species interactome differences, *Proc. Natl. Acad. Sci. USA* 103, 11527 (2006).
- [8] H. Jeong, S. Mason, A.-L. Barabási and Z. N. Oltvai, Lethality and centrality in protein networks, *Nature (London)* 411, 41 (2001).
- [9] A. Wagner, The Yeast Protein Interaction Network Evolves Rapidly and Contains Few Redundant Duplicate Genes, *Mol. Biol. Evol.* 18, 1283 (2001).
- [10] S. Y. Yook, Z. N. Oltvai, and A.-L. Barabási, Functional and topological characterization of protein interaction networks, *Proteomics* 4, 928 (2004).
- [11] A. Rzhetsky and S. M. Gomez, Birth of scale-free molecular networks and the number of distinct DNA and protein domains per genome, *Bioinformatics* 17, 988, (2001); J. Qian, N. M. Luscombe, and M. Gerstein, Protein family and fold occurrence in genomes: Power-law behaviour and evolutionary model, *J. Mol. Biol.* 313, 673 (2001); A. Bhan, D. J. Galas, and T. G. Dewey, A duplication growth model of gene expression networks, *Bioinformatics* 18, 1486, (2002); R. V. Sole, R. Pastor-Satorras, E. Smith, and T. B. Kepler, A model of large-scale proteome evolution, *Adv. Complex Syst.* 5, 43, (2002); A. Vazquez, A. Flammini, A. Maritan, and A. Vespignani, Modeling of protein interaction networks, *Complexity* 1, 38, (2003).
- [12] J. Kim, P. L. Krapivsky, B. Kahng, and S. Redner, Infinite-order percolation and giant fluctuations in a protein interaction network, *Phys. Rev. E* 66, 055101(R) (2002); R. Pastor-Satorras, E. Smith, and R. V. Sole, Evolving protein interaction networks through gene duplication, *J. Theor. Biol.* 222, 199 (2003); I. Ispolatov, P. L. Krapivsky, and A. Yuryev, Duplication-divergence model of protein interaction network, *Phys. Rev. E* 71, 061911 (2005).
- [13] A.-L. Barabási and Z. N. Oltvai, Network biology: understanding the cells functional organization, *Nature Reviews Genetics* 5, 101 (2004).
- [14] J. Janin, Protein-protein recognition, *Prog. Biophys. Mol. Biol.* 64, 145 (1995).
- [15] A. Tamura and P. L. Privalov, The entropy cost of protein association, *J. Mol. Biol.* 273, 1048 (1997).
- [16] J. Estojak, R. Brent, and E. A. Golenis, Correlation of 2-hybrid affinity data with in-vitro measurements, *Mol. Cell. Biol.* 15, 5820 (1995).
- [17] N. Masuda, H. Miwa, and N. Konno, Analysis of scale-free networks based on a threshold graph with intrinsic vertex weights, *Phys. Rev. E* 70, 036124 (2004);
- [18] M. Boguna and R. Pastor-Satorras, Class of correlated random networks with hidden variables, *Phys. Rev. E* 68, 036112 (2003).
- [19] C. M. Deane, L. Salwinski, I. Xenarios, D. Eisenberg, Protein interactions – Two methods for assessment of the reliability of high throughput observations, *Mol. Cell. Proteomics* 1, 349 (2002).
- [20] G. Caldarelli, A. Capocci, P. De Los Rios, and M. A. Muñoz, Scale-free networks from varying vertex intrinsic fitness, *Phys. Rev. Lett.* 89, 258702 (2002).
- [21] D. Balcan and A. Erzan, Random model for RNA interference yields scale free network, *Euro. Phys. J.* 38, 253 (2004).